SANDIA REPORT

SAND2005-4237
Unlimited Release
Printed July 2005

Explicit A Posteriori Error Estimates for Eigenvalue Analysis of Heterogeneous Elastic Structures

T. F. Walsh, G. M. Reese, and U. L. Hetmaniuk

Prepared by
Sandia National Laboratories
Albuquerque, New Mexico 87185 and Livermore, California 94550

Sandia is a multiprogram laboratory operated by Sandia Corporation,
a Lockheed Martin Company, for the United States Department of Energy's
National Nuclear Security Administration under Contract DE-AC04-94-AL85000.

Sandia National Laboratories

Issued by Sandia National Laboratories, operated for the United States Department of Energy by Sandia Corporation.

Printed in the United States of America. This report has been reproduced directly from the best available copy.

Available to DOE and DOE contractors from
U.S. Department of Energy
Office of Scientific and Technical Information
P.O. Box 62
Oak Ridge, TN 37831

Telephone:	(865) 576-8401
Facsimile:	(865) 576-5728
E-Mail:	reports@adonis.osti.gov
Online ordering:	http://www.doe.gov/bridge

Available to the public from
U.S. Department of Commerce
National Technical Information Service
5285 Port Royal Rd
Springfield, VA 22161

Telephone:	(800) 553-6847
Facsimile:	(703) 605-6900
E-Mail:	orders@ntis.fedworld.gov
Online ordering:	http://www.ntis.gov/help/ordermethods.asp?loc=7-4-0#online

SAND2005-4237
Unlimited Release
Printed July 2005

Explicit A Posteriori Error Estimates for Eigenvalue Analysis of Heterogeneous Elastic Structures

Timothy F. Walsh and Garth M. Reese
Computational Solid Mechanics and Structural Dynamics

Ulrich L. Hetmaniuk
Computational Mathematics and Algorithms

Sandia National Laboratories
P.O. Box 5800
Albuquerque, NM 87185

Abstract

An a posteriori error estimator is developed for the eigenvalue analysis of three-dimensional heterogeneous elastic structures. It constitutes an extension of a well-known explicit estimator to heterogeneous structures. We prove that our estimates are independent of the variations in material properties and independent of the polynomial degree of finite elements. Finally, we study numerically the effectivity of this estimator on several model problems.

Explicit A Posteriori Error Estimates for Eigenvalue Analysis of Heterogeneous Elastic Structures

Contents

Figures

Tables

1 Introduction

Eigenvalue analysis is common in many areas of engineering. For example, the knowledge of the eigenspectrum of a linear structure allows an analyst to decide whether an excitation frequency will be close to a resonance frequency, which could cause vibrations of large amplitude. The eigenpairs of a linear structure can also determine efficiently, in a linear superposition procedure, its transient or frequency response. For large scale heterogeneous structures, where the finite element models reach ten millions or more degrees of freedom, researchers at Sandia National Labs [12] frequently compute thousands of eigenmodes. In order to have confidence in the accuracy of these modes and to adaptively refine the mesh, quantifying the discretization error is important and a posteriori error analysis becomes critical.

A posteriori error estimation has received considerable attention over the last three decades. Recent reviews [1, 15, 16] give excellent summaries and background on the subject. Unfortunately, as far as eigenvalue analysis is concerned, a posteriori error estimators are less studied than the estimators for traditional static elliptic or time-dependent problems. Therefore, the aim of this paper is to analyze an a posteriori error estimator in the context of structural eigenanalysis without damping but with heterogeneities.

Verfürth [14] has proved the equivalence between an explicit estimator and the errors on the eigenvalue and the eigenvector, while using a general framework for non-linear equations with the assumption that the computed eigenpair is close to the continuous eigensolution. Under the same assumption, Larson [7] recently introduced explicit a priori and a posteriori estimates for the eigensolution of the scalar elliptic operators. For smooth eigenvectors, Larson's estimates bounded the errors in eigenvalues and eigenvectors in terms of the element-wise residuals, the mesh size, and a stability factor. Heuveline and Rannacher [6] extended the work of Larson [7] to unsymmetric operators by representing the eigenvalue problem in the more general framework of a nonlinear variational problem. Unfortunately, their least-squares approach requires the a priori knowledge of the smoothness of the continuous solution and it provides only upper bounds of the error [1]. Requiring the a priori knowledge of the smoothness is a disadvantage that makes these estimates impractical for general three-dimensional structures.

Oden et al. [11] used the so-called *goal-oriented* error estimation approach, also commonly referred to as the *quantity of interest* error estimation approach. Choosing the eigenvalue as a quantity of interest, their approach defined an implicit error estimate at the element level, which eliminates the typical unknown constant present in explicit estimators. But bubble spaces must be used for the local linear solves.

For piecewise linear elements and for the Laplacian operator, Duran et al. [5] proved that a simple explicit, residual-based estimator was equivalent to the error in the eigenvectors, up to higher order terms. They also proved that the error was equivalent to the jump term in the element level residual, and thus eliminated the interior residual term from the estimator. Their approach is close to the one used in this paper for treating the elasticity equation with higher degree elements.

The previously described estimators do not consider the common case of heterogeneous materials in structural analysis. The goal of this paper is to analyze an explicit residual-based estimator that treats the case of high order finite elements and can also handle discontinuous material coefficients. Our approach follows closely the work of Araya and Le Tallec [2] and the analysis of Bernardi and Verfürth [4], which considered source problems.

The outline of the paper goes as follows. In section 2, we present the model problem. In section 3, we recall some known a priori error estimates for its finite element approximation. In section 4, we define the explicit estimator and prove its equivalence with the error in the eigenfunction up to high order terms. We give also an upper bound on the error for eigenvalues. Finally, numerical examples illustrate the effectivity of this estimator.

2 Model problem and notations

Let $\Omega \subset \mathbb{R}^3$ be a bounded domain, with Lipschitz continuous boundary $\Gamma = \Gamma_D \cup \Gamma_N$, $\Gamma_D \cap \Gamma_N = \emptyset$, and $\mathrm{meas}(\Gamma_D) > 0$.

We consider the eigenvalue problem: find $(\mathbf{u}, \theta)$ such that

$$-\nabla \cdot \boldsymbol{\sigma}(\mathbf{u}) = \theta \rho \mathbf{u} \quad \text{in } \Omega, \tag{1a}$$

$$\mathbf{u} = \mathbf{0} \quad \text{on } \Gamma_D, \tag{1b}$$

$$\boldsymbol{\sigma}(\mathbf{u}) \cdot \mathbf{n} = \mathbf{0} \quad \text{on } \Gamma_N. \tag{1c}$$

The stress tensor $\boldsymbol{\sigma}(\mathbf{u})$ is related to the strain tensor $\boldsymbol{\varepsilon}(\mathbf{u})$,

$$\boldsymbol{\varepsilon}(\mathbf{u}) = \begin{bmatrix} \partial_1 u_1 \\ \partial_2 u_2 \\ \partial_3 u_3 \\ (\partial_3 u_2 + \partial_2 u_3)/2 \\ (\partial_3 u_1 + \partial_1 u_3)/2 \\ (\partial_2 u_1 + \partial_1 u_2)/2 \end{bmatrix}, \tag{2}$$

by the material law

$$\boldsymbol{\sigma}(\mathbf{u}) = \mathbf{D}\boldsymbol{\varepsilon}(\mathbf{u}), \tag{3}$$

where $\mathbf{D}$ is a function with values in symmetric positive definite matrices satisfying the property

$$0 < d_{\min} \mathbf{y}^T \mathbf{y} \leq \mathbf{y}^T \mathbf{D}(x) \mathbf{y} \leq d_{\max} \mathbf{y}^T \mathbf{y}, \quad \forall\, x \in \Omega. \tag{4}$$

We assume that the density function ρ is bounded

$$0 < \rho_{\min} \leq \rho(x) \leq \rho_{\max}, \quad \forall\, x \in \Omega. \tag{5}$$

Such a Sturm-Liouville problem has an infinite sequence of real eigenvalues

$$0 < \theta_1 \leq \theta_2 \leq \cdots \leq \theta_j \leq \cdots \to \infty,$$

and an associated complete set of orthonormal eigenfunctions

$$\int_{\Omega} \rho \mathbf{u}_j \cdot \mathbf{u}_k dx = \delta_{jk}.$$

We define also a weak formulation: find $(\mathbf{u}, \theta) \in H^1_{\Gamma_D}(\Omega) \times \mathbb{R}$

$$a(\mathbf{u}, \mathbf{v}) = \theta b(\mathbf{u}, \mathbf{v}), \quad \forall\, \mathbf{v} \in H^1_{\Gamma_D}(\Omega), \tag{6a}$$

$$b(\mathbf{u}, \mathbf{u}) = 1, \tag{6b}$$

where

$$a(\mathbf{u}, \mathbf{v}) = \int_{\Omega} \boldsymbol{\sigma}(\mathbf{u}) \cdot \boldsymbol{\varepsilon}(\mathbf{v}) dx = \int_{\Omega} \boldsymbol{\varepsilon}(\mathbf{u})^T \mathbf{D} \boldsymbol{\varepsilon}(\mathbf{v}) dx, \tag{7a}$$

$$b(\mathbf{u}, \mathbf{v}) = \int_{\Omega} \rho \mathbf{u} \cdot \mathbf{v} dx, \tag{7b}$$

and

$$H^1_{\Gamma_D}(\Omega) = \left\{ \mathbf{v} \in H^1(\Omega) \mid \mathbf{v} = \mathbf{0} \text{ on } \Gamma_D \right\}. \tag{8}$$

Note that the bilinear form a is symmetric, coercive, and continuous. The form a satisfies

$$C(\Omega, \Gamma_D) d_{\min} \|\mathbf{v}\|^2_{H^1(\Omega)} \leq a(\mathbf{v}, \mathbf{v}), \tag{9a}$$

$$a(\mathbf{u}, \mathbf{v}) \leq d_{\max} \|\mathbf{u}\|_{H^1(\Omega)} \|\mathbf{v}\|_{H^1(\Omega)}. \tag{9b}$$

Remark 1. *When the domain Ω is homogeneous and isotropic, we have*

$$\mathbf{D} = \begin{bmatrix} \lambda + 2\mu & \lambda & \lambda & 0 & 0 & 0 \\ \lambda & \lambda + 2\mu & \lambda & 0 & 0 & 0 \\ \lambda & \lambda & \lambda + 2\mu & 0 & 0 & 0 \\ 0 & 0 & 0 & 2\mu & 0 & 0 \\ 0 & 0 & 0 & 0 & 2\mu & 0 \\ 0 & 0 & 0 & 0 & 0 & 2\mu \end{bmatrix}, \tag{10}$$

where the Lamé constants λ and μ satisfy

$$\lambda = \frac{\nu E}{(1+\nu)(1-2\nu)} \quad , \quad \mu = \frac{E}{2(1+\nu)}. \tag{11}$$

The eigenvalues of $\mathbf{D}$ *are*

$$\{3\lambda + 2\mu,\ 2\mu,\ 2\mu,\ 2\mu,\ 2\mu,\ 2\mu\}. \tag{12}$$

When $E > 0$ and $1/2 > \nu \geq 0$, we have

$$d_{\min} = 2\mu, \quad d_{\max} = 3\lambda + 2\mu, \quad \textit{and} \quad \frac{d_{\max}}{d_{\min}} = \frac{1+\nu}{1-2\nu}. \tag{13}$$

3 The discrete problem

3.1 Finite element discretization

Let $\mathcal{T}_h$, $h > 0$, be a family of partitions of Ω into tetrahedra or hexahedra. Each partition $\mathcal{T}_h$ must be consistent with Γ_D and Γ_N, i.e. Γ_D and Γ_N are the union of faces of elements of $\mathcal{T}_h$. We write, for any element K, $h_K = \mathrm{diam}(K)$ and, for any face F, $h_F = \mathrm{diam}(F)$. We denote by $\mathcal{F}_h$ the set of all faces in $\mathcal{T}_h$. $\mathcal{F}_h$ naturally splits into the sets $\mathcal{F}_{h,\Omega}$, $\mathcal{F}_{h,D}$, and $\mathcal{F}_{h,N}$ of all faces in Ω, Γ_D, and Γ_N, respectively.

Over each element K, we introduce a suitable space of polynomials $Q^p(K)$ of degree smaller than p. We always demand that the degrees of freedom are suitably constrained so that an approximation function $\mathbf{v}_h$ is continuous over Ω and that $\mathbf{v}_h$ satisfies the Dirichlet boundary condition. This construction leads to a space of piecewise polynomial functions $V_h^p \subset H^1_{\Gamma_D}(\Omega)$.

3.2 A priori error analysis

The finite element approximate solutions are defined by: find $(\mathbf{u}_h, \theta_h) \in V_h^p \times \mathbb{R}$ such that

$$a(\mathbf{u}_h, \mathbf{v}_h) = \theta_h b(\mathbf{u}_h, \mathbf{v}_h), \quad \forall\, \mathbf{v}_h \in V_h^p, \tag{14a}$$

$$b(\mathbf{u}_h, \mathbf{u}_h) = 1. \tag{14b}$$

This approximate problem reduces to a generalized eigenvalue problem involving symmetric definite positive matrices, which admits strictly positive eigenvalues

$$0 < \theta_{h,1} \leq \theta_{h,2} \leq \ldots \leq \theta_{h,N_h}. \tag{15}$$

A priori error estimation for eigenvalue problems is well documented in [3, 13]. The a priori estimates provide convergence rates for finite element approximation of eigenvalues and eigenvectors.

Theorem 1. *Let assume that, for an arbitrary eigenpair $(\mathbf{u}, \theta)$ of problem (6), the eigenvector belongs to $H^s(\Omega)$ $(s > 1)$. There exists a constant C, independent of h, such that, for h sufficiently small, an approximate eigenpair $(\mathbf{u}_h, \theta_h)$ satisfies the estimates*

$$\theta \leq \theta_h \leq \theta + C\frac{h^{2\min(s,p+1)-2}}{p^{2s-2}} \tag{16a}$$

$$\sqrt{a(e,e)} \leq C\frac{h^{\min(s,p+1)-1}}{p^{s-1}} \tag{16b}$$

$$\sqrt{b(e,e)} \leq C\frac{h^{\min(s,p+1)}}{p^{s}} \tag{16c}$$

$$\tag{16d}$$

Note that the constant C depends on the eigenvalue θ, the domain, and the mesh regularity. An interesting result is that the eigenvalues converge at twice the rate for the eigenvectors in the energy norm. These results will be used later to define the higher order terms in the estimates and also to verify the convergence rates predicted by the a posteriori error estimators.

4 Explicit a posteriori error estimates

We introduce an error estimator and prove its equivalence with the error up to higher order terms. The approach is similar to the ones described in [4, 5].

Assumptions

We assume in this section that the functions $\mathbf{D}$ and ρ are piecewise constant, i.e. $\mathbf{D}$ and ρ are constant on each element K. In addition, we assume that the family of partitions $\mathcal{T}_h$ is regular enough to allow the following result.

Assumption 1. *There exist two positive constants c_{I1} and c_{I2} depending only on the mesh regularity and a linear operator*

$$\mathbf{I}_h : \; H^1_{\Gamma_D}(\Omega) \to V_h^p \tag{17}$$

such that for any $\mathbf{v} \in H^1_{\Gamma_D}(\Omega)$, for any element K, and for any face F

$$\|\mathbf{v} - \mathbf{I}_h(\mathbf{v})\|_{L^2(K)} \leq c_{I1} \frac{h_K}{p\sqrt{d_{K,\min}}} \sqrt{\int_{\omega_K} \boldsymbol{\sigma}(\mathbf{v}) \cdot \boldsymbol{\varepsilon}(\mathbf{v})} \tag{18a}$$

$$\|\mathbf{v} - \mathbf{I}_h(\mathbf{v})\|_{L^2(F)} \leq c_{I2} \sqrt{\frac{h_F}{d_{F,\min} p}} \sqrt{\int_{\omega_F} \boldsymbol{\sigma}(\mathbf{v}) \cdot \boldsymbol{\varepsilon}(\mathbf{v})} \tag{18b}$$

where the patch ω_K (resp. ω_F) contains the element K (resp. the face F). $d_{K,\min}$ denotes here the smallest eigenvalue of $\mathbf{D}$ over the element K. $d_{F,\min}$ is equal to $\min(d_{K_1,\min}, d_{K_2,\min})$, with K_1 and K_2 the two elements adjacent to F.

Note that each element K and each face F is contained in a fixed finite number of patches ω_K and ω_F. Similar estimates have been proven in Bernardi and Verfürth [4] (see lemma 2.8 where $p = 1$) and in Muñoz-Sola [10] (for the Laplacian operator).

Notations

With each face F in $\mathcal{F}_{h,\Omega}$, we associate a unit normal $\mathbf{n}_F$ and denote by $J_F(\phi)$ the jump of a given function ϕ across F in direction $\mathbf{n}_F$. We set

$$R_K(\mathbf{u}_h, \theta_h) = \nabla \cdot \boldsymbol{\sigma}(\mathbf{u}_h) + \theta_h \rho \mathbf{u}_h, \quad K \in \mathcal{T}_h, \tag{19a}$$

$$R_F(\mathbf{u}_h) = \begin{cases} J_F(\mathbf{n}_F \cdot \boldsymbol{\sigma}(\mathbf{u}_h)), & F \in \mathcal{F}_{h,\Omega}, \\ \mathbf{n}_F \cdot \boldsymbol{\sigma}(\mathbf{u}_h), & F \in \mathcal{F}_{h,N}, \\ \mathbf{0}, & F \in \mathcal{F}_{h,D}. \end{cases} \tag{19b}$$

Let the global error estimator η be

$$\left\{ \sum_{K \in \mathcal{T}_h} \frac{h_K^2}{d_{K,\min} p^2} \|R_K(\mathbf{u}_h, \theta_h)\|^2_{L^2(K)} + \sum_{F \in \mathcal{F}_h} \frac{h_F}{d_{F,\min} p} \|R_F(\mathbf{u}_h)\|^2_{L^2(F)} \right\}^{\frac{1}{2}}. \tag{20}$$

Finally, for the sake of abbreviation, we denote

$$a_K(\mathbf{u},\mathbf{v}) = \int_K \boldsymbol{\sigma}(\mathbf{u})\cdot\boldsymbol{\varepsilon}(\mathbf{v}), \quad \|\mathbf{u}\|_{a,K} = a_K(\mathbf{u},\mathbf{u})^{1/2},$$

and

$$b_K(\mathbf{u},\mathbf{v}) = \int_K \rho\mathbf{u}\cdot\mathbf{v}, \quad \|\mathbf{u}\|_{b,K} = b_K(\mathbf{u},\mathbf{u})^{1/2}.$$

4.1 Global upper bound for eigenvectors

For any eigenpair $(\mathbf{u},\theta)$ and an approximate solution $(\mathbf{u}_h,\theta_h)$, we denote the error function $\mathbf{e} = \mathbf{u}-\mathbf{u}_h$. We assume the following properties

$$\left\{\begin{array}{rcl} a(\mathbf{u},\mathbf{u}) &=& \theta, \\ b(\mathbf{u},\mathbf{u}) &=& 1, \end{array}\right. \quad \left\{\begin{array}{rcl} a(\mathbf{u}_h,\mathbf{u}_h) &=& \theta_h, \\ b(\mathbf{u}_h,\mathbf{u}_h) &=& 1. \end{array}\right.$$

We start by giving some general results.

Lemma 1. *We have*

$$b(\theta\mathbf{u}-\theta_h\mathbf{u}_h,\mathbf{e}) = \frac{\theta+\theta_h}{2}b(\mathbf{e},\mathbf{e}). \tag{21}$$

Proof. We expand the left hand side of (21)

$$\begin{array}{rcl} b(\theta\mathbf{u}-\theta_h\mathbf{u}_h,\mathbf{e}) &=& b(\theta\mathbf{u}-\theta_h\mathbf{u}_h,\mathbf{u}) - b(\theta\mathbf{u}-\theta_h\mathbf{u}_h,\mathbf{u}_h), \\ b(\theta\mathbf{u}-\theta_h\mathbf{u}_h,\mathbf{e}) &=& \theta+\theta_h-(\theta+\theta_h)b(\mathbf{u},\mathbf{u}_h), \end{array}$$

where we used the normalization property. We now expand the right hand side of (21)

$$\begin{array}{rcl} b(\mathbf{e},\mathbf{e}) &=& b(\mathbf{u},\mathbf{u}) - 2b(\mathbf{u},\mathbf{u}_h) + b(\mathbf{u}_h,\mathbf{u}_h), \\ b(\mathbf{e},\mathbf{e}) &=& 2-2b(\mathbf{u},\mathbf{u}_h). \end{array}$$

Combining these two expansions, we get

$$\begin{array}{rcl} b(\theta\mathbf{u}-\theta_h\mathbf{u}_h,\mathbf{e}) &=& \theta+\theta_h-(\theta+\theta_h)(1-\frac{1}{2}b(\mathbf{e},\mathbf{e})), \\ b(\theta\mathbf{u}-\theta_h\mathbf{u}_h,\mathbf{e}) &=& \dfrac{\theta+\theta_h}{2}b(\mathbf{e},\mathbf{e}). \end{array}$$

□

Lemma 2. *For any* $\mathbf{v}\in H^1_{\Gamma_D}(\Omega)$, *we have*

$$a(\mathbf{e},\mathbf{v}) - b(\theta\mathbf{u}-\theta_h\mathbf{u}_h,\mathbf{v}) = \sum_{K\in\mathcal{T}_h}\int_K (\nabla\cdot\boldsymbol{\sigma}(\mathbf{u}_h)+\theta_h\rho\mathbf{u}_h)\cdot\mathbf{v} - \sum_{F\in\mathcal{F}_{h,N}}\int_F \mathbf{n}\cdot\boldsymbol{\sigma}(\mathbf{u}_h)\cdot\mathbf{v} - \sum_{F\in\mathcal{F}_{h,\Omega}}\int_F J_F(\mathbf{n}\cdot\boldsymbol{\sigma}(\mathbf{u}_h))\cdot\mathbf{v}. \tag{22}$$

Proof. For any $\mathbf{v} \in H^1_{\Gamma_D}(\Omega)$, we have

$$a(\mathbf{e}, \mathbf{v}) = \sum_{K \in \mathcal{T}_h} \int_K \boldsymbol{\sigma}(\mathbf{e}) \cdot \boldsymbol{\varepsilon}(\mathbf{v}).$$

Integrating by parts over K, we obtain

$$\begin{aligned}
a(\mathbf{e}, \mathbf{v}) &= \sum_{K \in \mathcal{T}_h} \int_K (-\nabla \cdot \boldsymbol{\sigma}(\mathbf{u}) + \nabla \cdot \boldsymbol{\sigma}(\mathbf{u}_h)) \cdot \mathbf{v} + \sum_{K \in \mathcal{T}_h} \int_{\partial K} \mathbf{n} \cdot \boldsymbol{\sigma}(\mathbf{e}) \cdot \mathbf{v}, \\
a(\mathbf{e}, \mathbf{v}) &= \sum_{K \in \mathcal{T}_h} \int_K (-\nabla \cdot \boldsymbol{\sigma}(\mathbf{u}) - \theta_h \rho \mathbf{u}_h + \nabla \cdot \boldsymbol{\sigma}(\mathbf{u}_h) + \theta_h \rho \mathbf{u}_h) \cdot \mathbf{v} \\
&\quad + \sum_{K \in \mathcal{T}_h} \int_{\partial K} \mathbf{n} \cdot \boldsymbol{\sigma}(\mathbf{e}) \cdot \mathbf{v}.
\end{aligned}$$

To simplify the last expression, we use the following properties of the eigenvector

$$\left\{ \begin{array}{rcll}
-\nabla \cdot \boldsymbol{\sigma}(\mathbf{u}) &=& \theta \rho \mathbf{u} & \text{in } \Omega \\
\mathbf{n} \cdot \boldsymbol{\sigma}(\mathbf{u}) &=& \mathbf{0} & \text{on } \Gamma_N \\
J_F(\mathbf{n} \cdot \boldsymbol{\sigma}(\mathbf{u})) &=& \mathbf{0} & \text{on } F \in \mathcal{F}_{h,\Omega}.
\end{array} \right.$$

We obtain

$$\begin{aligned}
a(\mathbf{e}, \mathbf{v}) = \sum_{K \in \mathcal{T}_h} \int_K \rho(\theta \mathbf{u} - \theta_h \mathbf{u}_h) \cdot \mathbf{v} + \sum_{K \in \mathcal{T}_h} \int_K (\nabla \cdot \boldsymbol{\sigma}(\mathbf{u}_h) + \theta_h \rho \mathbf{u}_h) \cdot \mathbf{v} \\
- \sum_{F \in \mathcal{F}_{h,N}} \int_F \mathbf{n} \cdot \boldsymbol{\sigma}(\mathbf{u}_h) \cdot \mathbf{v} - \sum_{F \in \mathcal{F}_{h,\Omega}} \int_F J_F(\mathbf{n} \cdot \boldsymbol{\sigma}(\mathbf{u}_h)) \cdot \mathbf{v}.
\end{aligned}$$

□

We state now the upper bound result.

Proposition 1. *The energy norm of the error satisfies*

$$\sqrt{a(\mathbf{e}, \mathbf{e})} \leq C\eta + \frac{\theta + \theta_h}{2} \frac{b(\mathbf{e}, \mathbf{e})}{\sqrt{a(\mathbf{e}, \mathbf{e})}} \tag{23}$$

where the constant C depends on Ω, Γ_D, and the regularity of $\mathcal{T}_h$.

Proof. For any $\mathbf{w}_h$ in V_h^p, we have

$$\begin{aligned}
a(\mathbf{e}, \mathbf{e}) &= a(\mathbf{e}, \mathbf{e} - \mathbf{w}_h) + a(\mathbf{e}, \mathbf{w}_h) \\
a(\mathbf{e}, \mathbf{e}) &= a(\mathbf{e}, \mathbf{e} - \mathbf{w}_h) + a(\mathbf{u}, \mathbf{w}_h) - a(\mathbf{u}_h, \mathbf{w}_h) \\
a(\mathbf{e}, \mathbf{e}) &= a(\mathbf{e}, \mathbf{e} - \mathbf{w}_h) + b(\theta \mathbf{u} - \theta_h \mathbf{u}_h, \mathbf{w}_h) \\
a(\mathbf{e}, \mathbf{e}) &= a(\mathbf{e}, \mathbf{e} - \mathbf{w}_h) - b(\theta \mathbf{u} - \theta_h \mathbf{u}_h, \mathbf{e} - \mathbf{w}_h) + b(\theta \mathbf{u} - \theta_h \mathbf{u}_h, \mathbf{e})
\end{aligned}$$

We use equations (21, 22).

$$a(\mathbf{e},\mathbf{e}) \;=\; \sum_{K\in\mathcal{T}_h}\int_K R_K(\mathbf{u}_h,\theta_h)\cdot(\mathbf{e}-\mathbf{w}_h) - \sum_{F\in\mathcal{F}_h}\int_F R_F(\mathbf{u}_h)\cdot(\mathbf{e}-\mathbf{w}_h) + \frac{\theta+\theta_h}{2}b(\mathbf{e},\mathbf{e})$$

Using the Cauchy-Schwarz inequality and inserting relations (18), we obtain

$$\begin{aligned}
a(\mathbf{e},\mathbf{e}) &\leq \sum_{K\in\mathcal{T}_h} c_{I1}\frac{h_K}{p\sqrt{d_{K,\min}}}\|R_K(\mathbf{u}_h,\theta_h)\|_{L^2(K)}\|\mathbf{e}\|_{a,\omega_K} \\
&\quad + \sum_{F\in\mathcal{F}_h} c_{I2}\sqrt{\frac{h_F}{d_{F,\min}p}}\|R_F(\mathbf{u}_h)\|_{L^2(F)}\|\mathbf{e}\|_{a,\omega_F} + \frac{\theta+\theta_h}{2}b(\mathbf{e},\mathbf{e}) \\
a(\mathbf{e},\mathbf{e}) &\leq \max(c_{I1},c_{I2})\eta\left\{\sum_{K\in\mathcal{T}_h}\|\mathbf{e}\|^2_{a,\omega_K} + \sum_{F\in\mathcal{F}_h}\|\mathbf{e}\|^2_{a,\omega_F}\right\}^{\frac{1}{2}} + \frac{\theta+\theta_h}{2}b(\mathbf{e},\mathbf{e}) \\
a(\mathbf{e},\mathbf{e}) &\leq C\eta\sqrt{a(\mathbf{e},\mathbf{e})} + \frac{\theta+\theta_h}{2}b(\mathbf{e},\mathbf{e})
\end{aligned}$$

$\square$

Remark 2. *In equation (23), the term*

$$\frac{\theta+\theta_h}{2}\frac{b(\mathbf{e},\mathbf{e})}{\sqrt{a(\mathbf{e},\mathbf{e})}}$$

is a higher order term. Asymptotically, we have

$$\frac{\theta+\theta_h}{2}\frac{b(\mathbf{e},\mathbf{e})}{\sqrt{a(\mathbf{e},\mathbf{e})}} = \mathcal{O}\left(\frac{h^{\min(s,p+1)+1}}{p}\right).$$

Remark 3. *Defining the estimator $\tilde{\eta}$ as*

$$\left\{\sum_{K\in\mathcal{T}_h}\frac{h_K^2}{d_{K,\max}p^2}\|R_K(\mathbf{u}_h,\theta_h)\|^2_{L^2(K)} + \sum_{F\in\mathcal{F}_h}\frac{h_F}{d_{F,\max}p}\|R_F(\mathbf{u}_h)\|^2_{L^2(F)}\right\}^{\frac{1}{2}}, \tag{24}$$

the energy norm of the error satisfies also

$$\sqrt{a(\mathbf{e},\mathbf{e})} \leq C\sqrt{\frac{d_{\max}}{d_{\min}}}\tilde{\eta} + \frac{\theta+\theta_h}{2}\frac{b(\mathbf{e},\mathbf{e})}{\sqrt{a(\mathbf{e},\mathbf{e})}} \tag{25}$$

where the constant C depends on Ω, Γ_D, and the regularity of $\mathcal{T}_h$.

4.2 Auxiliary results

With each element $K \in \mathcal{T}_h$ and each face $F \in \mathcal{F}_h$, we associate a bubble function ψ_K and ψ_F, as in [15]. Note that ψ_K is bounded by 1 and vanishes outside of K. Similarly, ψ_F is bounded by 1 and vanishes outside of $\hat{\omega}_F$, the union of all elements having F as a face.

Proposition 2. *Given an arbitrary integer k, there are constants $\gamma_1, \ldots, \gamma_5$, which only depend on k and the regularity of the mesh $\mathcal{T}_h$, such that the inequalities on an element K*

$$\|\mathbf{v}\|_{L^2(K)} \leq \gamma_1 \|\psi_K^{1/2}\mathbf{v}\|_{L^2(K)} \tag{26a}$$

$$|\psi_K \mathbf{v}|_{H^1(K)} \leq \gamma_2 h_K^{-1} \|\mathbf{v}\|_{L^2(K)} \tag{26b}$$

and on a face F

$$\|\mathbf{w}\|_{L^2(F)} \leq \gamma_3 \|\psi_F^{1/2}\mathbf{w}\|_{L^2(F)} \tag{27a}$$

$$|\psi_F \mathbf{w}|_{H^1(\hat{\omega}_F)} \leq \gamma_4 h_F^{-1/2} \|\mathbf{w}\|_{L^2(F)} \tag{27b}$$

$$\|\psi_F \mathbf{w}\|_{L^2(\hat{\omega}_F)} \leq \gamma_5 h_F^{1/2} \|\mathbf{w}\|_{L^2(F)} \tag{27c}$$

hold for all $K \in \mathcal{T}_h$, all $F \in \mathcal{F}_h$, and all polynomials $\mathbf{v}$, $\mathbf{w}$ of degree at most k defined on K and $\hat{\omega}_F$, respectively.

Proof. See [15] and the references therein. □

Melenk and Wohlmuth [8] show also how the coefficients γ_i depend on the degree k in $\mathbb{R}^2$.

4.3 Local lower bound for eigenvectors

Proposition 3. *For any element K in $\mathcal{T}_h$, we have*

$$\frac{h_K}{p}\|R_K(\mathbf{u}_h, \theta_h)\|_{L^2(K)} \leq C_1\sqrt{d_{K,\max}}\|\mathbf{e}\|_{a,K} + C_2 h_K \sqrt{\rho_K}\|\theta\mathbf{u} - \theta_h\mathbf{u}_h\|_{b,K} \tag{28}$$

where the positive constants C_1 and C_2 depend on p and the regularity of the mesh. ρ_K denotes the value of ρ on the element K.

Proof. Consider the bubble function

$$\mathbf{w}_K = \psi_K R_K(\mathbf{u}_h, \theta_h).$$

Using (26a), we have

$$\begin{aligned}
\|R_K(\mathbf{u}_h, \theta_h)\|^2_{L^2(K)} &\leq \gamma_1^2 \int_K \psi_K |R_K(\mathbf{u}_h, \theta_h)|^2 \\
\|R_K(\mathbf{u}_h, \theta_h)\|^2_{L^2(K)} &\leq \gamma_1^2 \int_K (\nabla \cdot \boldsymbol{\sigma}(\mathbf{u}_h) + \theta_h \rho \mathbf{u}_h) \cdot \mathbf{w}_K \\
\|R_K(\mathbf{u}_h, \theta_h)\|^2_{L^2(K)} &\leq \gamma_1^2 \int_K (-\boldsymbol{\sigma}(\mathbf{u}_h) \cdot \boldsymbol{\varepsilon}(\mathbf{w}_K) + \rho\theta_h \mathbf{u}_h \cdot \mathbf{w}_K) \\
\|R_K(\mathbf{u}_h, \theta_h)\|^2_{L^2(K)} &\leq \gamma_1^2 \int_K \boldsymbol{\sigma}(\mathbf{e}) \cdot \boldsymbol{\varepsilon}(\mathbf{w}_K) + \gamma_1^2 \int_K \rho(\theta_h \mathbf{u}_h - \theta\mathbf{u}) \cdot \mathbf{w}_K
\end{aligned}$$

Using Cauchy-Schwarz inequalities for a_K and b_K, we have

$$\|R_K(\mathbf{u}_h,\theta_h)\|^2_{L^2(K)} \le \gamma_1^2\|\mathbf{e}\|_{a,K}\|\mathbf{w}_K\|_{a,K} + \gamma_1^2\|\theta\mathbf{u}-\theta_h\mathbf{u}_h\|_{b,K}\sqrt{\rho_K}\|\mathbf{w}_K\|_{L^2(K)}$$

We use now the boundedness of ψ_K and the continuity property of a_K.

$$\begin{aligned}\|R_K(\mathbf{u}_h,\theta_h)\|^2_{L^2(K)} \le \gamma_1^2\|\mathbf{e}\|_{a,K}\sqrt{d_{K,\max}}|\mathbf{w}_K|_{H^1(K)}& \\ + \gamma_1^2\|\theta\mathbf{u}-\theta_h\mathbf{u}_h\|_{b,K}\sqrt{\rho_K}\|R_K(\mathbf{u}_h,\theta_h)\|_{L^2(K)}&\end{aligned}$$

Finally, using (26b), we get

$$\begin{aligned}\|R_K(\mathbf{u}_h,\theta_h)\|^2_{L^2(K)} \le \gamma_1^2\|\mathbf{e}\|_{a,K}\sqrt{d_{K,\max}}\frac{\gamma_2}{h_K}\|R_K(\mathbf{u}_h,\theta_h)\|_{L^2(K)}& \\ + \gamma_1^2\sqrt{\rho_K}\|\theta\mathbf{u}-\theta_h\mathbf{u}_h\|_{b,K}\|R_K(\mathbf{u}_h,\theta_h)\|_{L^2(K)}&\end{aligned}$$

□

Remark 4. *The term*

$$h_K\|\theta\mathbf{u}-\theta_h\mathbf{u}_h\|_{b,K}$$

is a higher order term. Indeed, we have

$$\begin{aligned}\|\theta\mathbf{u}-\theta_h\mathbf{u}_h\|^2_{b,\Omega} &= \theta^2+\theta_h^2-2\theta\theta_h b(\mathbf{u},\mathbf{u}_h),\\ \|\theta\mathbf{u}-\theta_h\mathbf{u}_h\|^2_{b,\Omega} &= \theta^2+\theta_h^2+\theta\theta_h(b(\mathbf{e},\mathbf{e})-2),\\ \|\theta\mathbf{u}-\theta_h\mathbf{u}_h\|^2_{b,\Omega} &= (\theta-\theta_h)^2+\theta\theta_h b(\mathbf{e},\mathbf{e}).\end{aligned}$$

Asymptotically, we get

$$h_K\|\theta\mathbf{u}-\theta_h\mathbf{u}_h\|_{b,K} \le h\|\theta\mathbf{u}-\theta_h\mathbf{u}_h\|_{b,\Omega} = \mathcal{O}\left(\frac{h^{\min(s,p+1)+1}}{p^s}\right).$$

Proposition 4. *For any face F in $\mathcal{F}_h$, we have*

$$\sqrt{\frac{h_F}{p}}\|R_F(\mathbf{u}_h)\|_{L^2(F)} \le C_1\sqrt{d_{\max}}\|\mathbf{e}\|_{a,\hat{\omega}_F} + C_2 h\sqrt{\rho_{\max}}\|\theta\mathbf{u}-\theta_h\mathbf{u}_h\|_{b,\hat{\omega}_F} \tag{29}$$

where the positive constants C_1 and C_2 depend on p and the regularity of the mesh. $\hat{\omega}_F$ is the union of all elements having F as a face.

Proof. Consider the bubble function

$$\mathbf{w}_F = \psi_F R_F(\mathbf{u}_h).$$

Using (27a), we have

$$\|R_F(\mathbf{u}_h)\|^2_{L^2(F)} \le \gamma_3^2 \int_F R_F(\mathbf{u}_h) \cdot \mathbf{w}_F$$

We insert now the relation (22).

$$\|R_F(\mathbf{u}_h)\|^2_{L^2(F)} \le \gamma_3^2 a_{\hat{\omega}_F}(\mathbf{e}, \mathbf{w}_F) + \gamma_3^2 b_{\hat{\omega}_F}(\theta_h \mathbf{u}_h - \theta \mathbf{u}, \mathbf{w}_F) - \sum_{K \subset \hat{\omega}_F} \gamma_3^2 \int_K R_K(\mathbf{u}_h, \theta_h) \cdot \mathbf{w}_F$$

Using Cauchy-Schwarz inequalities for $a_{\hat{\omega}_F}$ and $b_{\hat{\omega}_F}$, we obtain

$$\begin{aligned}\|R_F(\mathbf{u}_h)\|^2_{L^2(F)} \le \gamma_3^2 \|\mathbf{e}\|_{a,\hat{\omega}_F} \|\mathbf{w}_F\|_{a,\hat{\omega}_F} + \gamma_3^2 \|\theta_h \mathbf{u}_h - \theta \mathbf{u}\|_{b,\hat{\omega}_F} \|\mathbf{w}_F\|_{b,\hat{\omega}_F} \\ + \sum_{K \subset \hat{\omega}_F} \gamma_3^2 \|R_K(\mathbf{u}_h, \theta_h)\|_{L^2(K)} \|\mathbf{w}_F\|_{L^2(K)}\end{aligned}$$

$$\begin{aligned}\|R_F(\mathbf{u}_h)\|^2_{L^2(F)} \le \gamma_3^2 \|\mathbf{e}\|_{a,\hat{\omega}_F} \sqrt{d_{\max}} |\psi_F \mathbf{R}_F(\mathbf{u}_h)|_{H^1(\hat{\omega}_F)} \\ + \gamma_3^2 \|\theta_h \mathbf{u}_h - \theta \mathbf{u}\|_{b,\hat{\omega}_F} \sqrt{\rho_{\max}} \|\psi_F \mathbf{R}_F(\mathbf{u}_h)\|_{L^2(F)} \\ + \sum_{K \subset \hat{\omega}_F} \gamma_3^2 \|R_K(\mathbf{u}_h, \theta_h)\|_{L^2(K)} \|\psi_F \mathbf{R}_F(\mathbf{u}_h)\|_{L^2(F)}\end{aligned}$$

Finally, using (27b, 27c), we obtain

$$\begin{aligned}\|R_F(\mathbf{u}_h)\|^2_{L^2(F)} \le \gamma_3^2 \|\mathbf{e}\|_{a,\hat{\omega}_F} \gamma_4 h_F^{-1/2} \sqrt{d_{\max}} \|\mathbf{R}_F(\mathbf{u}_h)\|_{L^2(F)} \\ + \gamma_3^2 \|\theta_h \mathbf{u}_h - \theta \mathbf{u}\|_{b,\hat{\omega}_F} \sqrt{\rho_{\max}} \gamma_5 h_F^{1/2} \|\mathbf{R}_F(\mathbf{u}_h)\|_{L^2(F)} \\ + \sum_{K \subset \hat{\omega}_F} \gamma_3^2 \|R_K(\mathbf{u}_h, \theta_h)\|_{L^2(K)} \gamma_5 h_F^{1/2} \|\mathbf{R}_F(\mathbf{u}_h)\|_{L^2(F)}\end{aligned}$$

Since $h_F \le h_K \le h$, this estimate together with inequality (28) allows us to conclude the proof. $\square$

Collecting estimates (28, 29), we have thus proven the following lower bound on the error, for any element $K \in \mathcal{T}_h$,

$$\begin{aligned}\left\{ \frac{h_K^2}{d_{K,\min} p^2} \|R_K(\mathbf{u}_h, \theta_h)\|^2_{L^2(K)} + \sum_{F \subset \partial K} \frac{\alpha_F h_F}{d_{F,\min} p} \|R_F(\mathbf{u}_h)\|^2_{L^2(F)} \right\}^{1/2} \\ \le C \left(\sqrt{\frac{d_{\max}}{d_{\min}}} \|\mathbf{e}\|_{a,\hat{\omega}_K} + h \sqrt{\frac{\rho_{\max}}{d_{\min}}} \|\theta \mathbf{u} - \theta_h \mathbf{u}_h\|_{b,\hat{\omega}_K} \right) \quad (30)\end{aligned}$$

where $\alpha_F = \frac{1}{2}$, if $F \in \mathcal{F}_{h,\Omega}$, and $\alpha_F = 1$, otherwise. $\hat{\omega}_K$ is the union of all elements sharing a face with K. Therefore, η yields, up to higher order terms, global upper and local lower bounds on the error of an eigenvector.

4.4 Global upper bound for eigenvalues

We show that η yields, up to higher order terms, an upper bound on the error of eigenvalues.

Proposition 5. *The eigenvalue θ and its approximation θ_h satisfy*

$$0 \leq \theta_h - \theta \leq C\eta^2 + h.o.t. \tag{31}$$

where h.o.t denotes a higher order term

$$h.o.t. = C\eta \frac{\theta_h + \theta}{2} \frac{b(\mathbf{e}, \mathbf{e})}{\sqrt{a(\mathbf{e}, \mathbf{e})}} + \frac{\theta_h - \theta}{2} b(\mathbf{e}, \mathbf{e})$$

The constants C depend on Ω, Γ_D, and the regularity of $\mathcal{T}_h$.

Proof. We have seen previously that

$$b(\mathbf{e}, \mathbf{e}) = 2 - 2b(\mathbf{u}, \mathbf{u}_h).$$

Similarly, we have

$$a(\mathbf{e}, \mathbf{e}) = \theta + \theta_h - 2\theta b(\mathbf{u}, \mathbf{u}_h).$$

Therefore, we obtain

$$\theta_h - \theta = a(\mathbf{e}, \mathbf{e}) - \theta b(\mathbf{e}, \mathbf{e}). \tag{32}$$

Using (23), we bound the error

$$\begin{aligned}
\theta_h - \theta &\leq C\eta\sqrt{a(\mathbf{e}, \mathbf{e})} + \frac{\theta_h + \theta}{2} b(\mathbf{e}, \mathbf{e}) - \theta b(\mathbf{e}, \mathbf{e}) \\
\theta_h - \theta &\leq C\eta\sqrt{a(\mathbf{e}, \mathbf{e})} + \frac{\theta_h - \theta}{2} b(\mathbf{e}, \mathbf{e}) \\
\theta_h - \theta &\leq C^2\eta^2 + C\eta \frac{\theta_h + \theta}{2} \frac{b(\mathbf{e}, \mathbf{e})}{\sqrt{a(\mathbf{e}, \mathbf{e})}} + \frac{\theta_h - \theta}{2} b(\mathbf{e}, \mathbf{e})
\end{aligned}$$

□

Remark 5. *From relation (32), we can expect that the effectivity of the estimator η for the eigenvalue will be close to the square root of the effectivity for the eigenvector.*

5 Numerical results

In this section, we present the numerical results. We study the effectivity of the estimator η for the eigenvalues, *i.e.*

$$\frac{\theta\eta}{\theta_h - \theta},$$

for heterogeneous, isotropic, one-dimensional, and three-dimensional elastic beams.

To compute the eigenpairs, we use a combination of implicitly restarted Lanczos with a domain-decomposition linear solver, as described in [12].

5.1 A one-dimensional elastic beam

First we consider a beam of length $L = 10$ made of two materials. For the left half ($0 \le x \le 5$), the material parameters are (E_1, $\nu_1 = 0$, $\rho_1 = 10^{-1}$), while, for the right half ($5 \le x \le 10$), they are ($E_2 = 10^7$, $\nu_2 = 0$, $\rho_2 = \rho_1$). The beam is clamped at one end and free at the other.

The exact eigenvalues for this case are given by the following transcendental equation

$$\cos\left(\frac{L}{2}\sqrt{\frac{\theta\rho_1}{E_1}}\right)\cos\left(\frac{L}{2}\sqrt{\frac{\theta\rho_2}{E_2}}\right) = \sqrt{\frac{\rho_2 E_2}{\rho_1 E_1}}\sin\left(\frac{L}{2}\sqrt{\frac{\theta\rho_1}{E_1}}\right)\sin\left(\frac{L}{2}\sqrt{\frac{\theta\rho_2}{E_2}}\right). \tag{33}$$

When E_1 is equal to E_2 (*i.e.* the homogeneous case), all the eigenvectors are analytic. When the Young moduli differ, the eigenvectors belong to $H^{5/2}(\Omega)$ [9].

The mesh is uniform and matches the discontinuity for the Young modulus. A summary of the effectivity indices and convergence rates is given in Tables 1 and 2 for the first four eigenvalues when the mesh is refined and when E_1 is changed. In accordance with (31), the effectivity indices do not depend on the eigenvalue, nor on the Young modulus. However, there is a slight decrease with the polynomial degree.

With linear elements, the convergence rates are consistent with the a priori estimates (16). However, when the structure is heterogeneous ($E_1 \neq E_2$) and quadratic elements are used, the convergence rates are better than the ones given by the a priori estimates (16). We believe that this *superconvergence* results from the matching of the mesh with the discontinuity in E.

5.2 A three-dimensional elastic beam

Here we study an isotropic elastic beam made of three-dimensional hexahedral elements. Figure 1 describes the geometry of the beam for the depth and height equal to 1. We assume that

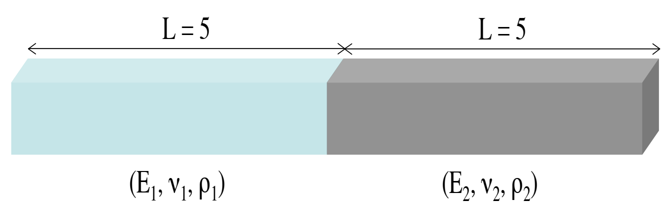

Figure 1. Three-dimensional heterogeneous elastic beam

the densities and Poisson ratios satisfy

$$\rho_1 = \rho_2 = 10^{-1} \text{ and } \nu_1 = \nu_2 = 0.$$

The Young modulus E_2 is set to 10^7 and we vary E_1. For these isotropic materials, we remark that jumps in density are equivalent to jumps in Young modulus. Therefore, we present results for jumps in Young modulus.

Eigenvalue λ_1

h	$E_1 = E_2$ Effectivity	Conv. Rate	$E_1 = 10^2 E_2$ Effectivity	Conv. Rate	$E_1 = 10^4 E_2$ Effectivity	Conv. Rate
1.0	22.7842	1.9627	27.0328	2.0743	22.7368	1.9631
.5	23.3975	1.9816	25.5247	2.0415	23.3820	1.9817
.25	23.6938	1.9909	24.7366	2.0219	23.7016	1.9909
.125	23.8670		24.3455		23.8572	

Eigenvalue λ_2

h	$E_1 = E_2$ Effectivity	Conv. Rate	$E_1 = 10^2 E_2$ Effectivity	Conv. Rate	$E_1 = 10^4 E_2$ Effectivity	Conv. Rate
1.0	22.6615	1.9639	23.8884	1.9961	22.3447	1.9702
.5	23.3599	1.9818	24.0003	1.9998	23.2463	1.9824
.25	23.6906	1.9909	24.0199	2.0006	23.6581	1.9910
.125	23.8420		24.0146		23.8393	

Eigenvalue λ_3

h	$E_1 = E_2$ Effectivity	Conv. Rate	$E_1 = 10^2 E_2$ Effectivity	Conv. Rate	$E_1 = 10^4 E_2$ Effectivity	Conv. Rate
1.0	22.4555	1.9673	23.4206	2.0082	22.2375	1.9930
.5	23.2914	1.9821	23.7436	1.9994	23.0150	1.9846
.25	23.6710	1.9910	23.9323	1.9997	23.5871	1.9912
.125	23.8415		23.9862		23.8246	

Eigenvalue λ_4

h	$E_1 = E_2$ Effectivity	Conv. Rate	$E_1 = 10^2 E_2$ Effectivity	Conv. Rate	$E_1 = 10^4 E_2$ Effectivity	Conv. Rate
1.0	22.2466	1.9742	24.0559	2.0369	21.9762	1.4348
.5	23.1949	1.9828	23.4837	2.0031	22.7822	1.9898
.25	23.6430	1.9910	23.8413	1.9999	23.5294	1.9916
.125	23.8351		23.9725		23.9724	

Table 1. Effectivity and convergence rates predicted by the estimator for the first four modes of the one-dimensional beam, using linear elements

Eigenvalue λ_1

	$E_1 = E_2$		$E_1 = 10^2 E_2$		$E_1 = 10^4 E_2$	
h	Effectivity	Conv. Rate	Effectivity	Conv. Rate	Effectivity	Conv. Rate
1.0	15.0314	4.0008	17.0846	4.0458	15.1094	4.0019
.5	15.0084	4.0001	16.4869	4.0240	15.0315	4.0008
.25	15.0031	4.0000	16.1989	4.0121	15.0086	4.0002
.125	14.8744		16.0590		15.0072	

Eigenvalue λ_2

	$E_1 = E_2$		$E_1 = 10^2 E_2$		$E_1 = 10^4 E_2$	
h	Effectivity	Conv. Rate	Effectivity	Conv. Rate	Effectivity	Conv. Rate
1.0	15.2787	4.0070	17.9285	4.0426	15.9287	4.0122
.5	15.0750	4.0021	16.8285	4.0281	15.2787	4.0069
.25	15.0194	4.006	16.3584	4.0138	15.0750	4.0022
.125	15.0048		16.1301		15.0194	

Eigenvalue λ_3

	$E_1 = E_2$		$E_1 = 10^2 E_2$		$E_1 = 10^4 E_2$	
h	Effectivity	Conv. Rate	Effectivity	Conv. Rate	Effectivity	Conv. Rate
1.0	15.7517	4.0171	19.5257	4.0222	17.2892	4.0109
.5	15.2067	4.0059	17.5794	4.0345	15.7518	4.0171
.25	15.0537	4.0017	16.7450	4.0170	15.2067	4.0059
.125	15.0137		16.2243		15.0537	

Eigenvalue λ_4

	$E_1 = E_2$		$E_1 = 10^2 E_2$		$E_1 = 10^4 E_2$	
h	Effectivity	Conv. Rate	Effectivity	Conv. Rate	Effectivity	Conv. Rate
1.0	16.4096	4.0275	22.1859	3.9519	18.6584	3.9566
.5	15.4007	4.0112	19.1225	4.0402	16.4098	4.0275
.25	15.1049	4.0032	17.7276	4.0214	15.4007	4.0112
.125	15.0267		16.7943		15.1049	

Table 2. Effectivity and convergence rates predicted by the estimator for the first four modes of the one-dimensional beam, using quadratic elements

No boundary condition is applied to the structure. Consequently, the beam can exhibit modes of bending, extension, torsion, or mixed type. We only consider quadratic elements, since linear elements are very poor at approximating bending and torsion responses. The mesh always matches the discontinuity in Young modulus.

In Figure 2, some bending, extension, and torsion modes are depicted, when E_1 is changed. Note that by symmetry of the beam, the bending mode has a multiplicity equal to 2. The estimator η detected the multiplicities, as it returned the same value for multiple eigenpairs.

A summary of the effectivity indices and point-by-point convergence rates is given in Table 3. We draw the following comments.

- The torsion modes are the most difficult modes to approximate. The approximation has not reached yet the asymptotic convergence.
- The estimator never underestimates the error.
- Within a class of modes (bending, extensional, or torsional), the effectivity behaves similarly.
- The effectivity for the extension mode is similar to the one-dimensional beam.
- Similarly to the one-dimensional beam, the convergence rates are better than the ones predicted by the a priori estimates (16).

Remark 6. *Computing the effectivity requires the values of the exact eigenvalues, which are not explicitly known. We obtained reliable approximate values by a Richardson extrapolation procedure.*

5.3 Effect of Poisson ratio

Equation (13) shows that the stability constant depends on the Poisson ratio. All of the previous numerical experiments involved materials with $\nu = 0$. In order to assess the effect of Poisson ratio on the estimator, we consider in this section the three-dimensional modes of the elastic beam with material parameters ($E = 10^7, \nu = 0.3, \rho = 10^{-1}$). In the incompressible limit, only the lower bound (30) for the estimator η degenerates.

Table 4 shows the point-by-point convergence rates and effectivity indices for the three-dimensional bar with $\nu = 0$ and $\nu = 0.3$. From the table, we draw the following conclusions.

- The estimator never underestimates the error.
- The convergence rates asymptotically approach 4.0.
- Within a class of modes (bending, extensional, or torsional), the effectivity behaves similarly.
- The efficiency for the extension mode is the most affected by the change in Poisson ratio.

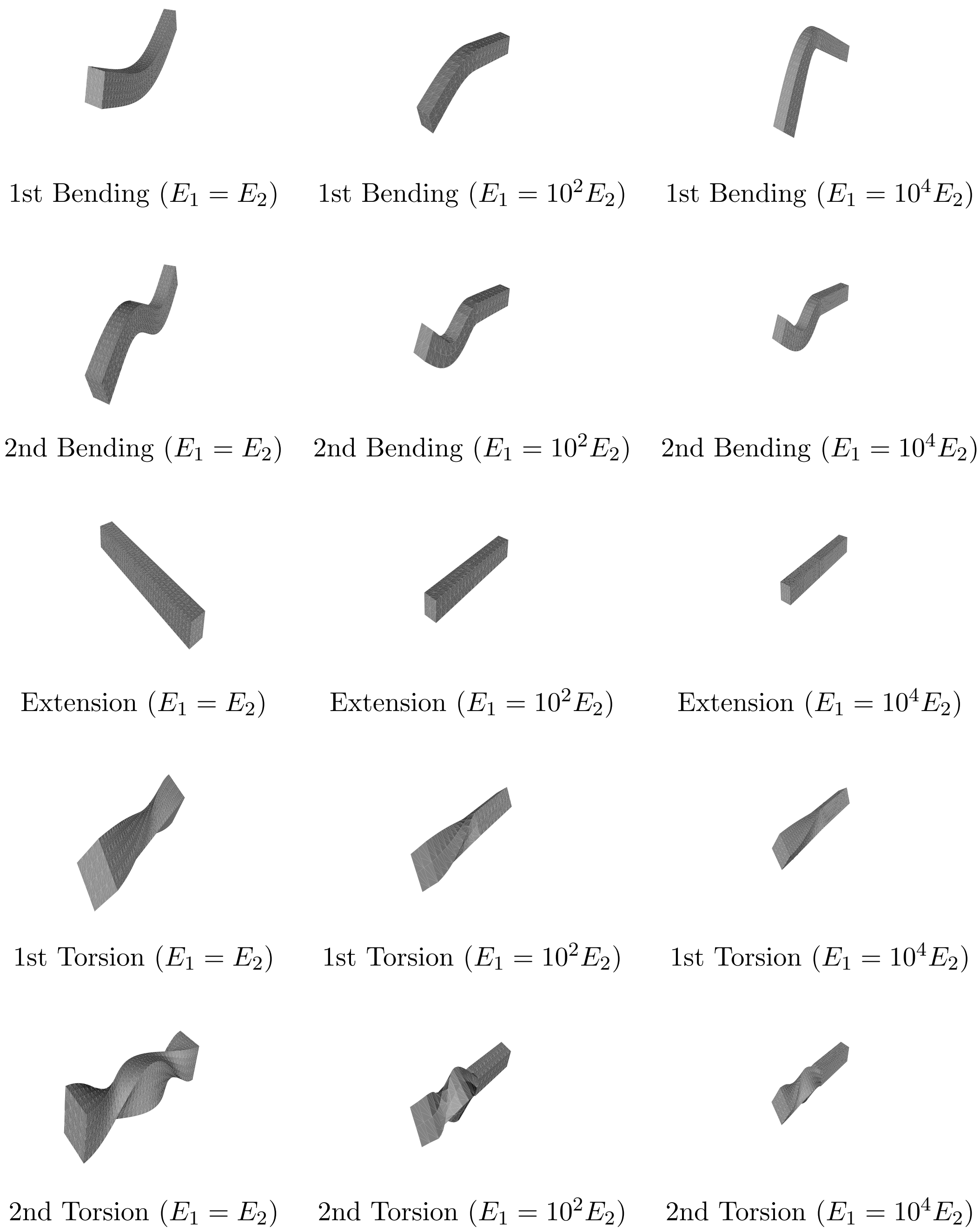

Figure 2. Modal shapes for three-dimensional beam

	First pair of bending modes					
	$E_1 = E_2$		$E_1 = 10^2 E_2$		$E_1 = 10^4 E_2$	
h	Effectivity	Conv. Rate	Effectivity	Conv. Rate	Effectivity	Conv. Rate
.5	7.7540	3.9767	7.2749	3.8042	7.2747	3.7472
.25	7.7558	3.9953	7.7080	3.8734	7.7085	3.8617
.125	7.7392	4.0003	7.8709	3.7846	7.9003	3.7671
.0625	7.7261		8.9662		9.1515	
	Second pair of bending modes					
	$E_1 = E_2$		$E_1 = 10^2 E_2$		$E_1 = 10^4 E_2$	
h	Effectivity	Conv. Rate	Effectivity	Conv. Rate	Effectivity	Conv. Rate
.5	7.7782	3.9419	7.3168	3.6928	7.3111	3.6275
.25	7.8882	3.9855	7.7663	3.7197	7.7826	3.7036
.125	7.8991	3.9975	8.1560	3.6441	8.1843	3.6261
.0625	7.8945		10.0327		10.0840	
	First extension mode					
	$E_1 = E_2$		$E_1 = 10^2 E_2$		$E_1 = 10^4 E_2$	
h	Effectivity	Conv. Rate	Effectivity	Conv. Rate	Effectivity	Conv. Rate
.5	15.0240	4.0007	15.8476	4.0380	15.8586	4.0026
.25	14.9312	4.0000	15.3856	4.0182	15.3980	4.0012
.125	14.9242	3.9992	15.1796	4.0086	15.3007	4.0004
.0625	14.9321		15.0857		15.2396	
	First torsion mode					
	$E_1 = E_2$		$E_1 = 10^2 E_2$		$E_1 = 10^4 E_2$	
h	Effectivity	Conv. Rate	Effectivity	Conv. Rate	Effectivity	Conv. Rate
.5	4.2465	3.2326	1.3799	1.7307	1.3814	1.9367
.25	5.6161	3.5800	4.2206	2.7388	4.2360	2.6770
.125	6.1417	3.6937	6.4223	2.9994	6.5031	2.8854
.0625	7.1905		11.5716		11.9608	
	Second torsion mode					
	$E_1 = E_2$		$E_1 = 10^2 E_2$		$E_1 = 10^4 E_2$	
h	Effectivity	Conv. Rate	Effectivity	Conv. Rate	Effectivity	Conv. Rate
.5	4.2799	3.2197	1.4320	1.6146	1.4351	1.8911
.25	5.6872	3.5835	4.2613	2.6325	4.2783	2.5770
.125	6.2080	3.6989	6.6576	2.9333	6.7468	2.8127
.0625	7.2429		12.4602		12.8818	

Table 3. Effectivity and convergence rates predicted by the estimator for the first modes of the three-dimensional beam, using quadratic elements

First pair of bending modes

	$\nu = 0$		$\nu = 0.3$	
h	Effectivity	Conv. Rate	Effectivity	Conv. Rate
.5	7.7540	3.9767	6.6520	3.5846
.25	7.7558	3.9953	8.1078	3.8813
.125	7.7392	4.0003	8.4089	3.9445
.0625	7.7261		8.6287	

Second pair of bending modes

	$\nu = 0$		$\nu = 0.3$	
h	Effectivity	Conv. Rate	Effectivity	Conv. Rate
.5	7.7782	3.9419	6.4904	3.4031
.25	7.8882	3.9855	8.6357	3.8180
.125	7.8991	3.9975	9.2163	3.9298
.0625	7.8945		9.5162	

First extension mode

	$\nu = 0$		$\nu = 0.3$	
h	Effectivity	Conv. Rate	Effectivity	Conv. Rate
.5	15.0240	4.0007	22.1362	3.7538
.25	14.9312	4.0000	24.4615	3.9208
.125	14.9242	3.9992	25.2414	3.9547
.0625	14.9321		25.8862	

First torsion mode

	$\nu = 0$		$\nu = 0.3$	
h	Effectivity	Conv. Rate	Effectivity	Conv. Rate
.5	4.2465	3.2326	1.3473	1.9692
.25	5.6161	3.5800	4.3447	3.2324
.125	6.1417	3.6937	5.7956	3.5850
.0625	7.1905		7.2552	

Second torsion mode

	$\nu = 0$		$\nu = 0.3$	
h	Effectivity	Conv. Rate	Effectivity	Conv. Rate
.5	4.2799	3.2197	1.3529	1.8408
.25	5.6872	3.5835	4.6548	3.2213
.125	6.2080	3.6989	6.2084	3.6013
.0625	7.2429		7.6723	

Table 4. Effect of Poisson ratio on effectivity and convergence rates predicted by the estimator for a homogeneous, isotropic, three-dimensional beam

6 Conclusions

In this paper, an a posteriori error estimator for eigenvalue analysis of three-dimensional elastic structures has been studied. This explicit estimator can deal with heterogeneous structures and high-order discretization. The estimator was tested with several model problems. It was verified that the convergence rates were consistent with a priori estimates and that the multiplicative constants were independent of jumps in material properties.

References

[1] Ainsworth, M. & Oden, J. T. (2000). *A posteriori error estimation in finite element analysis*. John Wiley & Sons, Inc.

[2] Araya, R. & Le Tallec, P. (1998). Adaptive finite element analysis for strongly heterogeneous elasticity problems. *Revue Européenne des Élements Finis 7*, 6: 635–655.

[3] Babuska, I. & Osborn, J. E. (1991). *Eigenvalue problems*. vol. 2. North-Holland. Amsterdam. 641–787.

[4] Bernardi, C. & Verfürth, R. (2000). Adaptive finite element methods for elliptic equations with non-smoooth coefficients. *Numerische Mathematik 85*: 579–608.

[5] Duran, R.; Padra, C. & Rodriguez, R. (2003). A posteriori error estimates for the finite element approximation of eigenvalue problems. *Mathematical Models and Methods in Applied Sciences 13*, 8: 1219–1229.

[6] Heuveline, V. & Rannacher, R. (2001). A posteriori error control for finite element approximations of elliptic eigenvalue problems. *Advances in Computational Mathematics 15*: 107–138.

[7] Larson, M. (2000). A posteriori and a priori error analysis for finite element approximations of self-adjoint elliptic eigenvalue problems. *SIAM Journal of Numerical Analysis 38*, 2: 608–625.

[8] Melenk, J. M. & Wohlmuth, B. I. (2001). On residual-based a posteriori error estimation in *hp*-FEM. *Advances in Computational Mathematics 15*: 311–331.

[9] Min, M. S. & Gottlieb, D. (2003). On the convergence of the Fourier approximation for eigenvalues and eigenfunctions of discontinuous problems. *SIAM Journal of Numerical Analysis 40*: 2254–2269.

[10] Muñoz-Sola, R. (1997). Polynomial liftings on a tetrahedron and applications to the $h-p$ version of the finite element method in three dimensions. *SIAM Journal of Numerical Analysis 34*, 1: 282–314.

[11] Oden, J. T.; Prudhomme, S.; Westermann, T.; Bass, J. & Botkin, M. E. (2003). Error estimation of eigenfrequencies for elasticity and shell problems. *Mathematical Models and Methods in Applied Sciences 13*, 3: 323–344.

[12] Reese, G. M. & Day, D. M. (1999). A massively parallel sparse eigensolver for structural dynamics finite element analysis. Tech. Rep. SAND99-1158. Sandia National Laboratories.

[13] Strang, G. & Fix, G. J. (1973). *An analysis of the finite element method*. Prentice-Hall.

[14] Verfürth, R. (1994). A posteriori error estimates for nonlinear problems. Finite element discretizations of elliptic equations. *Mathematics of Computation 62*: 445–475.

[15] Verfürth, R. (1996). *A review of a posteriori error estimation and adaptive mesh refinement techniques*. Wiley-Teubner.

[16] Verfürth, R. (1999). A review of a posteriori error estimation techniques for elasticity problems. *Computer Methods in Applied Mechanical Engineering 176*: 419–440.